High-contrast Metal-responsive Fluorescent Probes Based on Synergistic Electronic and Conformational Switching

A Thesis
Presented to
The Academic Faculty

by

Mysha Sarwar

In Partial Fulfillment
of the Requirements for the Bachelors of
Science Degree in Chemistry in the
School of Chemistry and Biochemistry

Georgia Institute of Technology
December 2011

High-contrast Metal-responsive Fluorescent Probes Based on Synergistic Electronic and Conformational Switching

Approved by:

Dr. Christoph Fahrni, Advisor
School of Chemistry and Biochemistry
Georgia Institute of Technology

Dr. Laren M. Tolbert
School of Chemistry & Biochemistry
Georgia Institute of Technology

Dr. William J. Baron
School of Chemistry & Biochemistry
Georgia Institute of Technology

Date Approved:

ACKNOWLEDGEMENTS

I would like to thank my advisor, Dr. Christoph J. Fahrni, for giving me the opportunity to work in his lab and for his support with many aspects of my research project. I would also like to thank Michael Thomas Morgan Jr. for helping me with my research. I am also grateful to Jonathan Hofmekler, Sumalekshmy Sarojini and Pritha Bagchi for their affection and support.

TABLE OF CONTENTS

ABSTRACT

We have prepared and characterized a Mg(II)-responsive fluorescent probe, constructed using a large tetradentate, 15-membered crown ether ligand and a 1,3,5-triaryl-substituted pyrazoline fluorophore. The photoinduced electron transfer (PET) driving force between the ligand and fluorophore controls the fluorescence contrast ratio when an analyte is bound to the probe. Previous studies have shown that the maximum obtainable fluorescence probes based on macrocyclic ligands was impaired due to ternary complex formation of the metal-ligand complex with the solvent molecules. We redesigned the metal ion receptor by incorporating the aniline ring into the ligand. We selected four fluoro substituents to increase the electron withdrawing ability of the 1-aryl-ring, yielding a very high (~4000-fold) fluorescence enhancement upon saturation with Mg(II) in acetonitrile. The quantum yield of this pyrazoline probe was found to be 79%. We expect that the described approach should be applicable for rationally designing high-contrast pyrazoline-based PET probes selective towards other metal cations as well.

INTRODUCTION

Cation-selective fluorescent probes have proven to be valuable tools to detect a wide range of metal ions with high sensitivity and selectivity, and found widespread applications in biological chemistry, cell biology, materials science, and environmental chemistry. A large class of fluorescent probes is composed of a metal binding unit, that guarantees selectivity towards the target ion, and an electronically decoupled fluorophore that translates metal binding into a fluorescence increase through a photoinduced electron transfer switching mechanism. The detection sensitivity of the probe critically depends on the fluorescence contrast between the analyte-bound and free form. Recent studies on Cu(I)-selective probes containing a thiaza crown moiety as metal receptor revealed that ternary complex formation impaired the maximum obtainable fluorescence contrast.[1] As illustrated with Scheme 1, metal binding to the crown receptor of (±)-**1** induces a large geometrical change in which the ortho-hydrogen atoms of the aniline ring sterically clash with the crown-ether backbone. Association with a solvent molecule alleviates these unfavorable interactions which in turn result in weakening of the metal-nitrogen bond and therefore increased fluorescence quenching due to an increased aniline donor potential.

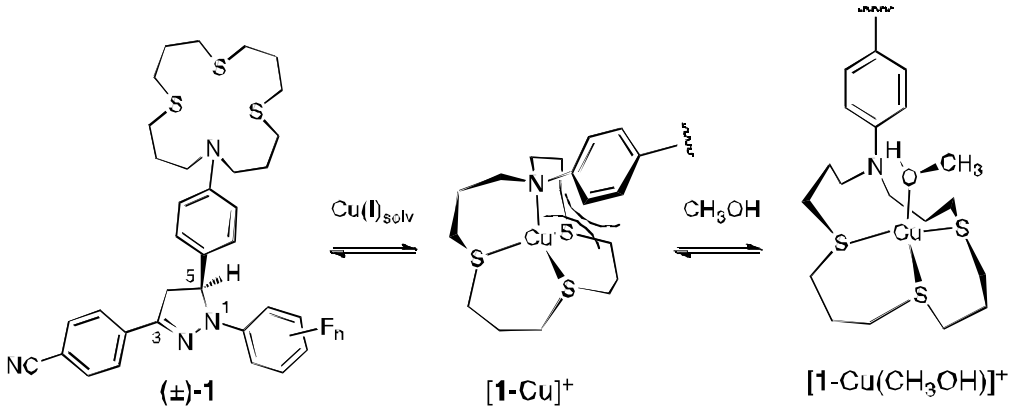

Scheme 1

These studies implied that similar quenching mechanisms might take place in structurally related aniline-based receptor architectures, which have been previously utilized for the construction of fluorescent probes selective towards alkali and alkaline earth metal ions. Theoretical studies on arylazacrown ethers and their complexes with Ca(II) indeed suggested the presence of multiple species including ternary complexes with solvent molecules.[1] Similarly, ternary complex formation appears responsible for a weakening of metal-nitrogen interaction, which in turn complicates the photophysical behavior through photoinduced recoordination.[2] To avoid the sterically unfavorable interactions, we redesigned the arylazacrown ether ligand **A** such that the aniline ring becomes an integral part of the ligand backbone (Scheme 2). Metal ion coordination to **B** is expected to promote a conformational change of at the aniline nitrogen while minimizing unfavorable steric interactions.

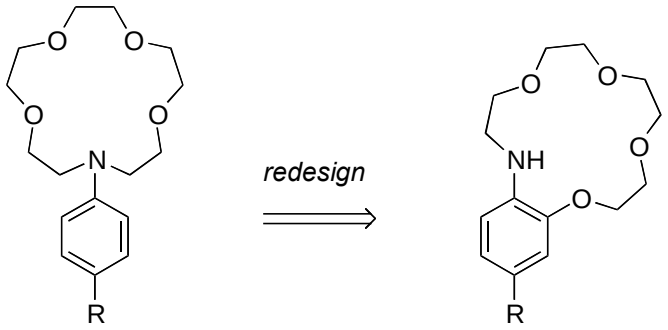

A **B**

Scheme 2

Ligands of type **B** principally allows for the design of a wide range of metal-ion responsive fluorescent probes. Taking advantage of the electronically tuneable pyrazoline fluorophores previously utilized,[2-4] we synthesized a metal-ion selective probe **2**.

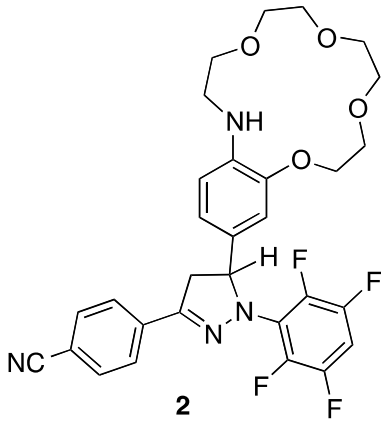

2

Based on our previously determined quantitative structure-property relationships of triaryl-pyrazoline probes,[1,4b] we selected four fluoro-substituents attached to the N-aryl ring of the pyrazoline fluorophore and optimized the fluorescence contrast as well as the switching

behavior of the probe. Furthermore, this compound was further characterized in terms of its photophysical properties as well as the binding affinities towards Mg^{2+} in acetonitrile.

PHOTOPHYSICAL BACKGROUND

The Photoinduced Electron Transfer (PET) process is a fluorescence quenching pathway that can be exploited to design cation selective fluorescence "turn on" probes.[3] When a fluorophore is excited, an electron moves from the Highest Occupied Molecular Orbital (HOMO) to the Lowest Unoccupied Molecular Orbital (LUMO) to produce an electronically excited state (S_1, Figure 1). In order for fluorescence to occur, the electron of the LUMO must return to the HOMO with emission of a photon. If an electron donating moiety is in close proximity to the fluorophore, then electron transfer can occur from the electron donor to fill the HOMO vacancy. The resulting electron transfer state decays non-radiatively to the ground state. Within a few picoseconds, the electron in the LUMO returns to the oxidized donor. Thus, an electron from the donor is transferred to the HOMO in the course of the PET process, yielding a charge separated electron transfer state (^{1}ET). Finally, charge recombination of two radical ion pair regenerates the original ground state (Figure 1).

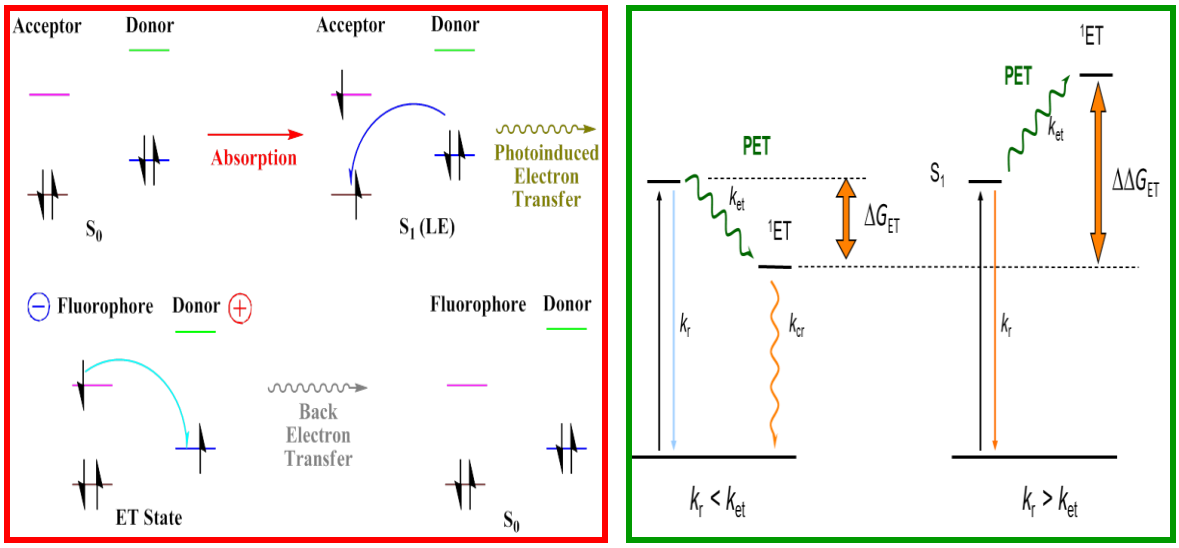

Figure 1: Photo-excitation of a fluorophore. Orbital energy diagram (left), Jablonski diagram (right). S_0 = ground state, S_1 = first excited singlet state, k_r = radiative rate constant, k_{et} = non-radiative electron transfer rate constant.

In absence of analytes in the system, when the fluorescent probe is not bound to any analyte, the PET process is energetically favorable as the ^{1}ET state is energetically lower than the first excited state (S_1). The PET process quenches fluorescence and thus we do not see any fluorescence upon exciting the molecule. However, when the analyte is bound to the ligand to form a tight metal-ligand complex, the electron density of the donor is less readily available to undergo the PET process. The electron transfer state shifts to higher energy and the PET process becomes energetically unfavorable. As a result, the fluorescence is switched on in an analyte-dependent manner.

Retrosynthetic Analysis of Fluorescent Probes 2

Scheme 3 illustrates the pertinent steps in the retrosynthetic analysis of the target fluorescent probe **2**. The pyrazoline core can be assembled through aldol condensation of aldehyde **7** with the acetophenone derivative **8**, followed by cyclization with the phenylhydrazine derivative **10**. Aldehyde **10** should be accessible through bromide **6** through halogen-lithium exchange at low temperature followed by quenching of the aryl anion with dimethylformamide. Furthermore, we anticipate that bromide **6** can be introduced through regio-selective bromination of ligand **5**, which in turn should be accessible through alkylation of 2-aminophenol **3** with the bis-chloroethylether **4**.

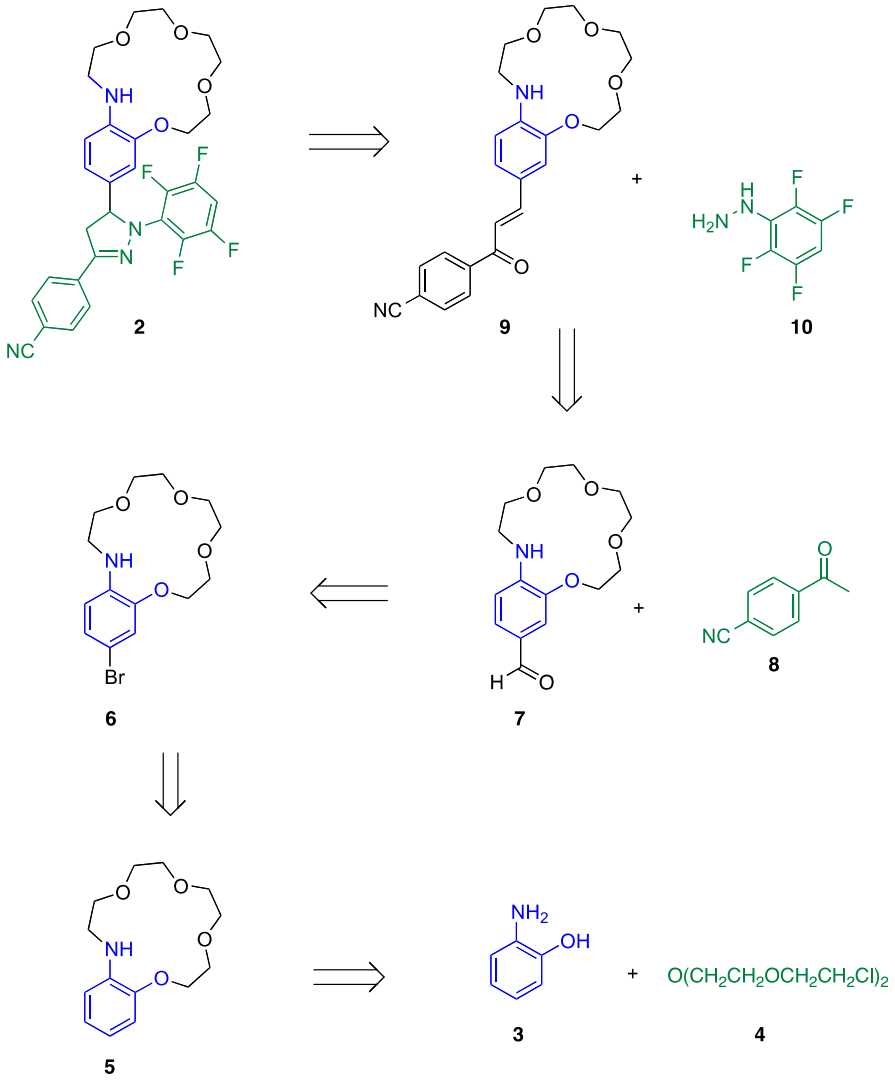

Scheme 3

MATERIALS AND METHODS

Bis(2-(2-chloroethoxy)ethyl)ether, 2-aminophenol, tetrabutylammonium tribromide, n-butyl lithium (2.5 M in hexanes), n-butyl lithium (2.5 M in hexanes), 4-acetylbenzonitrile, pyrrolidine, 2,3,5,6-tetrafluorophenylhydrazine, and pyridinium *p*-toluenesulfonate were purchased from Sigma-Aldrich. Melting points are uncorrected. Flash chromatography: Merck silica gel (70-230 mesh). TLC: 0.25 mm, Merck silica gel 60 F_{254}, visualizing at 254 nm or with 2% $KMnO_4$ solution.

3,5,6,8,9,11,12,13-Octahydro-2H-benzo[k][1,4,7,10,13]tetraoxaazacyclopentadecine (5):

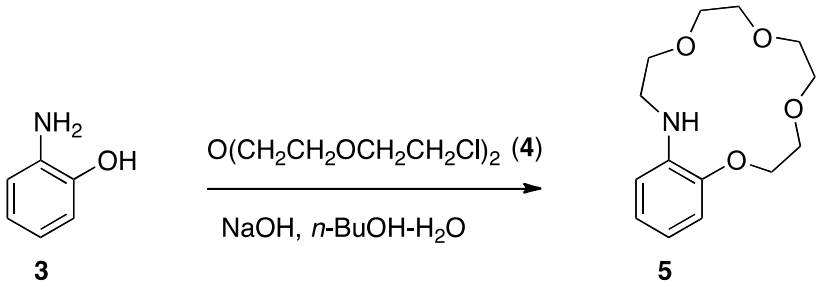

3 **5**

To a solution of 2-aminophenol **3** (8.55 g, 78 mmol) in n-BuOH (125 mL) bis(2-(2-chloroethoxy)ethyl)ether **4** (18.3 g, 79 mmol) was added. The mixture was heated at reflux under an atmosphere of N_2 for 18 hours. Then, the reaction was cooled down to 67 ºC and 6.33 g of NaOH (dissolved in 50 mL of H_2O) was added. The reaction was then refluxed under N_2 for 48 hours. After the starting material was completely converted (TLC), the solvent was evaporated and the crude solution was washed with 200 mL CH_2Cl_2 and 100 mL of 5% aqueous NaOH solution. The organic layer was dried with anhydrous $MgSO_4$, concentrated, and the residue purified by Kugelrohr distillation to give 2.49 g (9.3 mmol, 12% yield) of **5** as analytically pure product .

16-bromo-3,5,6,8,9,11,12,13-octahydro-2H-benzo[k][1,4,7,10,13]tetraoxaazacyclo-pentadecine (6):

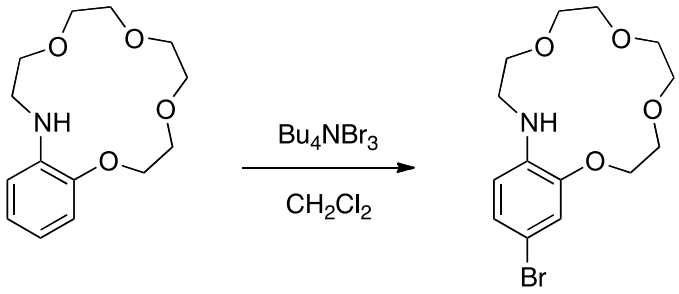

5 **6**

In a 1000 mL round bottom flask, 900 mg (3.36 mmol) of the macrocycle **5** was dissolved in dichloromethane (1 mL) and cooled in an ice bath under argon. A solution of tetrabutylammonium tribromide (1.623 g, 3.36 mmol) was added drop wise under stirring. Discoloration of the tribromide solution occurred. The mixture was stirred for 10 minutes at 0ºC and then at room temperature. The mixture was quenched with excess aqueous sodium sulfate. Mixture was diluted with water and MTBE. The organic layer was separated, washed with water and brine and then dried with anhydrous sodium sulfate. Without further purification 1.14 g (3.29 mmol, 95% yield) of pure product **6** was isolated.

3,5,6,8,9,11,12,13-octahydro-2H-benzo[k][1,4,7,10,13]tetraoxaazacyclopentadecine-16-carbaldehyde (7):

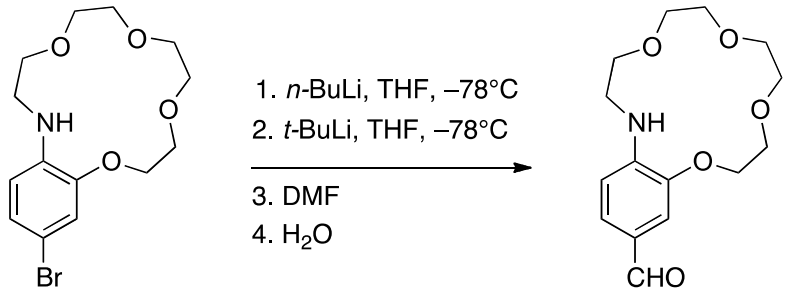

6 **7**

An oven dried 25 mL round bottom flask equipped with a magnetic stir bar was charged with bromide **6** (300 mg, 0.867 mmol), then sealed with a rubber septum and flushed with argon. Benzene (4 mL) was then added, and the resulting solution was concentrated to a viscous oil under a stream of argon in a 50°C oil bath. THF (6.2 mL) was then added, and after complete dissolution, the mixture was cooled in a dry ice-acetone bath (–78°C). A solution of *n*-butyl lithium (2.5 M in hexanes, 460 µL, 1.33 equiv.) was added dropwise to the stirred solution, and *tert*-butyl lithium solution (1.6 M in pentane, 1.08 mL, 2 equiv.) was then added in small portions over about 15 minutes. The mixture was stirred for a further 15 minutes at –78°C, and DMF (0.36 mL, 3 equiv.) was then added. The mixture was allowed to warm above 0°C, quenched with water (4 mL), stirred for several minutes, and then partitioned between water (25 mL) and dichloromethane (25 mL). The organic layer was separated, dried with anhydrous K_2CO_3, and concentrated under reduced pressure. The residue was subjected to column chromatography on silica gel (gradient, 1:2 hexane-dichloromethane plus increasing MTBE) to give aldehyde **7** as a pale brown oil. Yield 204 mg (0.69 mmol, 80%).

(E)-4-(3-(3,5,6,8,9,11,12,13-octahydro-2H-benzo[k][1,4,7,10,13] tetraoxaazacyclo pentadecan-16-yl)acryloyl)benzonitrile (8):

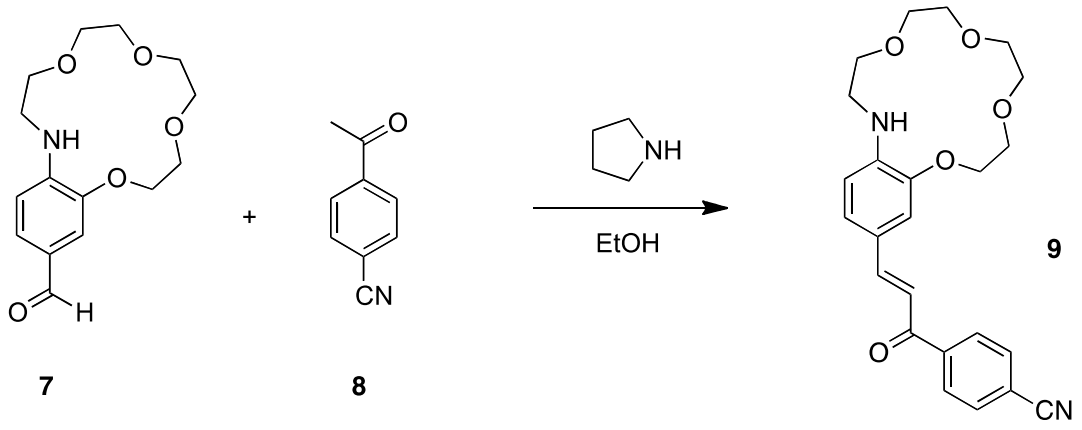

Aldehyde **7** (188 mg, 0.637 mmol) and 4-acetylbenzonitrile **8** (97 mg, 0.668 mmol, 1.05 equiv.) were dissolved in ethanol (1.0 mL) in a 10 mL pear shaped flask and pyrrolidine (53 µL, 1 equiv.) was then added. The mixture was stirred for 2 hours at room temperature and a further 2 hours at 45°C, then allowed to stand overnight at room temperature. A small patch of orange crystalline material formed in the neck of the flask and a larger amount of dark red gummy material settled at the bottom of the mixture. The crystalline material was scratched into the remainder of the mixture, which was then stirred at 45°C overnight. The resulting orange slurry was heated briefly to 70°C to dissolve a small remaining lump of gummy material, then allowed to cool to room temperature under slow stirring. The orange solid was filtered off, washed with cold ethanol, and recrystallized from toluene-cyclohexane under stirring to give the pure chalcone **9** as an orange crystalline powder. The yield was 130 mg (0.308 mmol, 48%) and the melting point was measured to be 144-145°C.

4-(5-(3,5,6,8,9,11,12,13-octahydro-2H-benzo[k] [1,4,7,10,13]tetraoxaazacyclopenta-decan-16-yl)-1-(2,3,5,6-tetrafluorophenyl)-4,5-dihydro-1H-pyrazol-3-yl)benzonitrile (2):

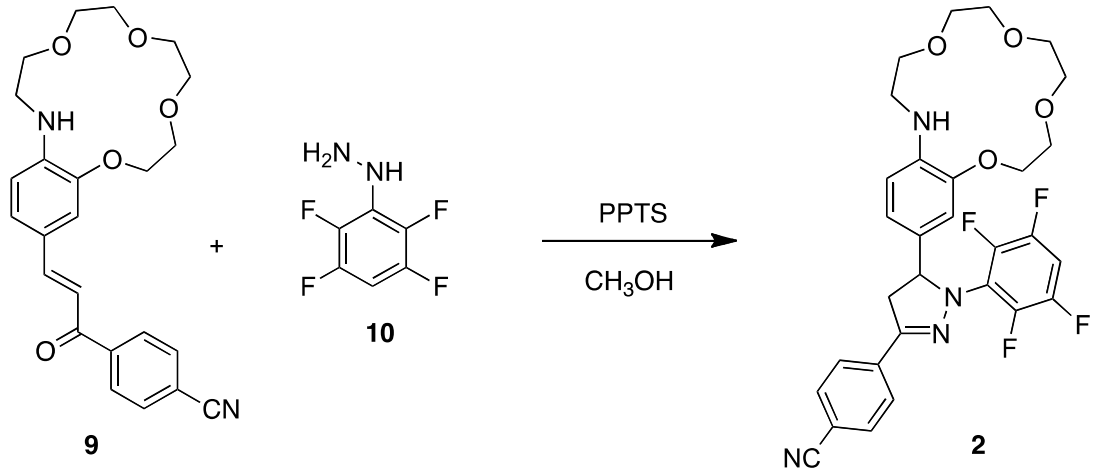

A 10 mL flask equipped with a magnetic stir bar was charged with chalcone **9** (52 mg, 0.123 mmol), 2,3,5,6-tetrafluorophenylhydrazine **10** (44 mg, 2 equiv.), pyridinium *p*-toluenesulfonate (62 mg, 2 equiv.) and methanol (1.2 mL), then flushed with argon and sealed with a Teflon stopper. The mixture was then stirred in an oil bath at 90°C. After 4 hours, the initial deep red color of the mixture had turned to light orange-brow, indicating consumption of the chalcone. The mixture was stirred at 90°C for a further 4 hours, allowed to cool, and concentrated to dryness. The residue was stirred with potassium carbonate (100 mg), water (2 mL), and toluene (6 mL), and the organic layer was then separated, washed with water (2 mL), dried with anhydrous potassium carbonate, filtered through cotton, and concentrated to dryness. The residue was subjected to column chromatography on silica gel (gradient, 1:1 hexane-dichloromethane plus increasing MTBE) to give product **2** in slightly impure form as yellow glassy solid (yield 56 mg, 78%). This material was dissolved in MTBE (500 µL), diluted with cyclohexane until a permanent turbidity remained, diluted slowly with MTBE until clear again, and stirred overnight to give a fine crystalline slurry. This was diluted further with MTBE (500 µL), heated briefly to boiling, then allowed to cool under slow stirring. The purified product was collected by filtration as a pale yellow-green powder (36 mg, 64% yield). Melting point was measured to be 143-144°C.

RESULTS AND DISCUSSION

1. Electrochemistry

To evaluate the redox properties of the Mg^{2+} coordinated to the crown ether receptor with improved ligand design, we conducted slow scan cyclic voltammetry studies in acetonitrile using magnesium perchlorate as the electrolyte at a concentration of 0.1 M. A solution of the ligand **5** showed in the presence of $Mg(ClO_4)_2$ an oxidation potential E_p = 1.3 V vs $Fc^{+/0}$, which is approximately 1.0 V higher compared to the free ligand (Figure 2). Furthermore, analysis of the commercially available disubstituted aniline crown ether ligand **11** revealed multiple oxidation waves, which are consistent with the presence of multiple ternary complexes formed as proposed Freidzon et al. based on molecular modeling studies.[6] Most importantly, ternary complex formation results in a switching potential for ligand **11** that is approximately 700 mV lower compared to the improved ligand design **5**.

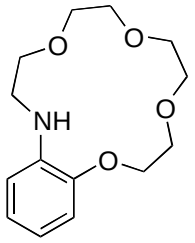

5

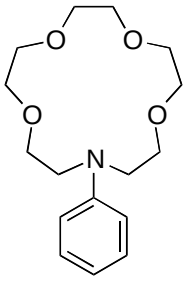

11

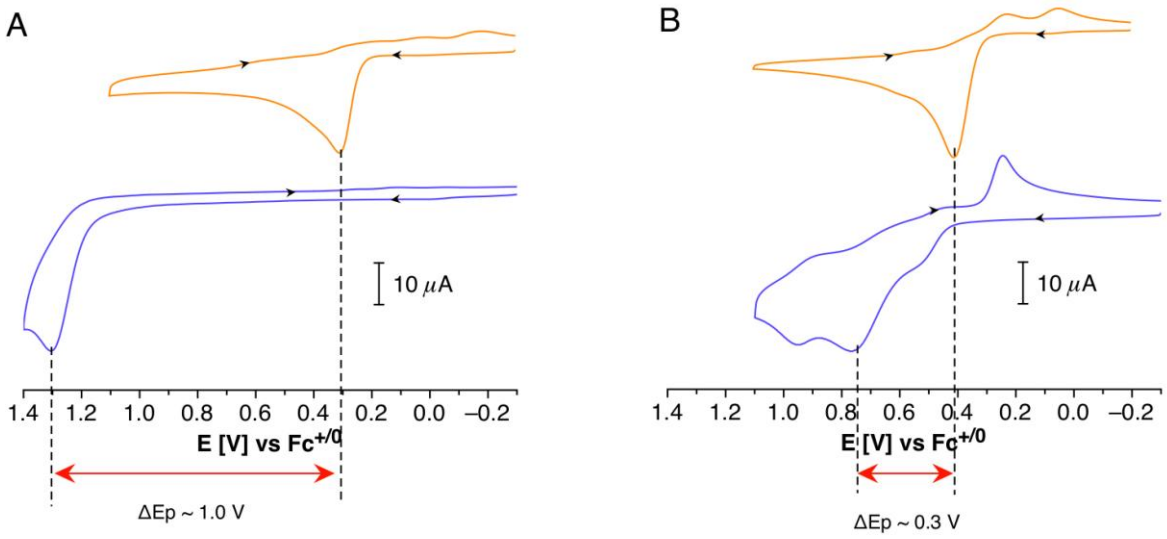

Figure 2: Cyclic voltammogram of ligands **5** and **11** in acetonitrile in the presence and absence of Mg(II)(ClO_4)$_2$. **A:** Comparison of the oxidation wave position of ligand **5** in its free form (yellow) and complexed with Mg(II) (blue trace). **B:** Comparison of the oxidation wave position of ligand **11** in its free form (yellow) and complexed with Mg(II) (blue trace).

2. Steady-State Absorption and Emission Spectroscopy

As illustrated with Figure 3A, the absorption spectrum of fluorescent probe **2** undergoes only a small red-shift upon binding of Mg(ClO_4)$_2$ in acetonitrile. This observation is consistent with exclusive binding to the crown ether moiety and only indirect electrostatic interaction with the pyrazoline fluorophore. In contrast the fluorescence of the metal-free probe is completely quenched and undergoes a greater than 4000-fold enhancement upon saturation with Mg(ClO_4)$_2$ (Figure 3B). The emission intensity reached saturation at an equimolar concentration of Mg(II), indicating formation of a complex with 1:1 metal-ligand stoichiometry.

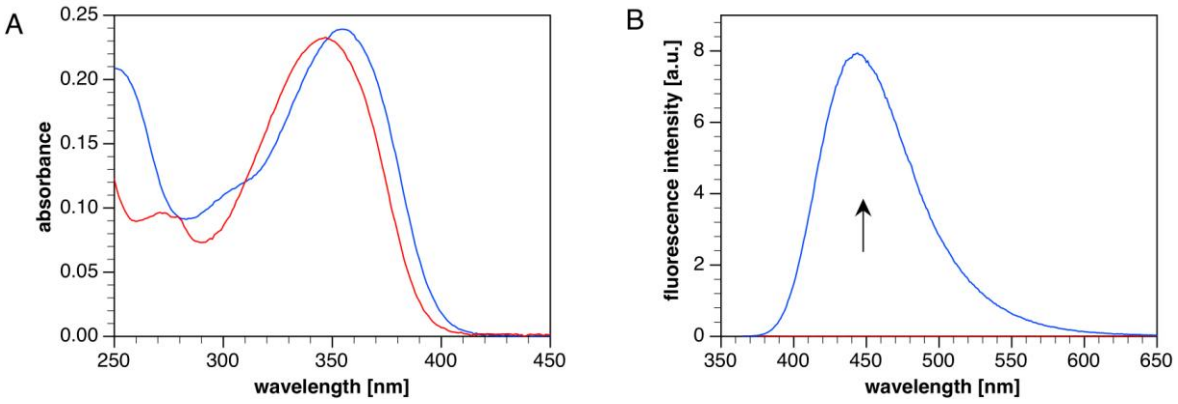

Figure 3: Spectral changes of fluorescent probe **2** (red traces) upon binding of Mg(II) (blue traces) in acetonitrile at 298K. **A**: Absorption spectra **B**: Fluorescence emission spectra with excitation at 350 nm.

3. Quantum Determination:

The quantum yield of compound **2** and the fluorescence enhancement factor upon saturation with 0.1 M $Mg(ClO_4)_2$ were determined in acetonitrile. For the quantum yield determination, the probe was excited at 380 nm and four data points with absorbances between 0.1 and 0.5 (l = 10 cm) were acquired. The following equation was used for a one point quantum yield determination in the case of fluorescence studies.

$$\Phi_x = \Phi_s * (A_x/A_s)*(I_x/I_s)*(n_x/n_s)^2$$

where Φ_x is the quantum yield of the unknown, Φ_s is the quantum yield of the standard, A_x is the optical density of the unknown, A_s is the optical density of the standard, I_x is the fluorescence intensity of the unknown, I_s is the fluorescence intensity of the standard and n_x is the refractive index of the medium of the unknown and n_s is the refractive index of the medium of the standard. Accordingly, the quantum yield of the Mg(II)-bound probe **2** was determined to be 79%. Given the approximately 4000-fold fluorescence enhancement factor, the quantum yield of the free ligand was estimated to be 0.02%.

4. Determination of the Mg(II) Binding Affinity

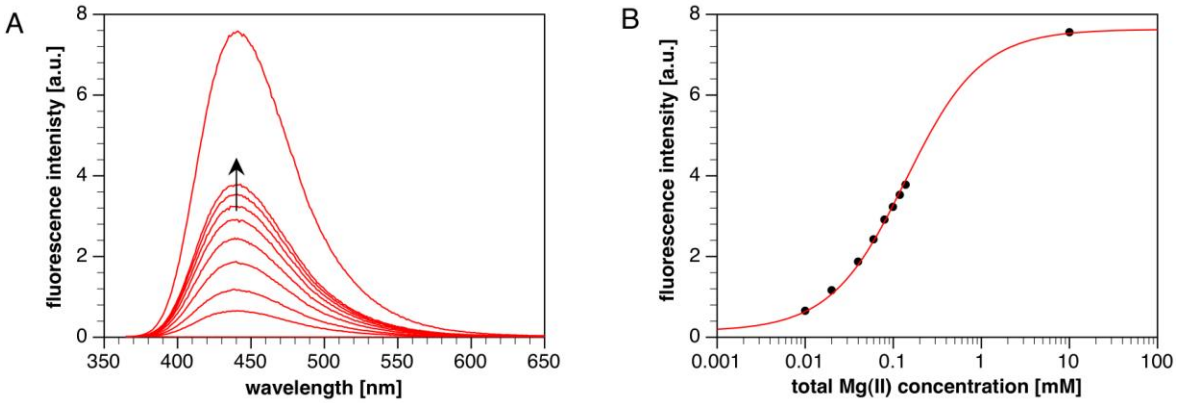

Figure 4: Fluorescence mol-ratio titration of probe **2** with $Mg(II)(ClO_4)_2$ in acetonitrile at 298K. A: Fluorescence emission spectral change with increasing concentration of Mg(II). B: Semi-log plot of the fluorescence intensity at 440 nm as a function of added Mg(II) (same data set as in panel A).

The binding affinity of the probe was determined through a molar-ratio titration as shown in Figure 4, and the fluorescence emission intensity at 440 nm was fitted according to the following formalism. The fluorescence response F of the probe **2** is given by

$$F = f_1 \times [\mathrm{L}] + f_2 \times [\mathrm{Mg(II)\,L}] \tag{1}$$

with [L] and [Mg(II)L] corresponding to the concentration of the free probe and its Mg(II) complex, respectively, and f_1 and f_2 are instrument-dependent proportionality factors. Assuming formation of a Mg(II) complex with 1:1 metal-ligand stoichiometry, the corresponding equilibrium binding constant K is defined by

$$K = \frac{[\mathrm{Mg(II)\,L}]}{[\mathrm{L}][\mathrm{Mg(II)}]} \tag{2}$$

Furthermore, we can define the total ligand $[L]_{tot}$ and magnesium $\{Mg(II)]_{tot}$ concentrations as

$$[L]_{tot} = [L] + [Mg(II)L] \quad \text{and} \tag{3}$$

$$[Mg(II)]_{tot} = [Mg(II)] + [Mg(II)L] \tag{4}$$

Solving equations (2-4) for [L] and [Mg(II)L] gives

$$[L] = \frac{f_1}{2}\left(2[L]_{tot} - [Mg(II)]_{tot} - K + \sqrt{K^2 - 4K[L]_{tot} + 2K[Mg(II)]_{tot} + [Mg(II)]_{tot}^2}\right) \tag{5}$$

and

$$[Mg(II)L] = \frac{1}{2}\left([Mg(II)]_{tot} + K - \sqrt{K^2 - 4K[L]_{tot} + 2K[Mg(II)]_{tot} + [Mg(II)]_{tot}^2}\right) \tag{6}$$

After insertion into equation (1), and the final fitting expression (7) is obtained which was used to extract the binding affinity K and the proportionality factors f_1 and f_2 by non-linear least squares fitting.

$$F = \frac{f_1}{2}\left(2[L]_{tot} - [Mg(II)]_{tot} - K + \sqrt{K^2 - 4K[L]_{tot} + 2K[Mg(II)]_{tot} + [Mg(II)]_{tot}^2}\right) + \frac{f_2}{2}\left([Mg(II)]_{tot} + K - \sqrt{K^2 - 4K[L]_{tot} + 2K[Mg(II)]_{tot} + [Mg(II)]_{tot}^2}\right) \tag{7}$$

The data yielded an excellent fit with K = 7500 ± 310 or K_d = 133 ± 5 uM for the Mg(II) affinity of probe **2** in acetonitrile.

CONCLUSIONS

We successfully addressed the adverse effects of ternary complex formation with the solvent molecules on the fluorescence switching behavior of cyclic crown-based donor-acceptor fluorescent probes by improving the ligand design. By integrating the aniline donor into the backbone of a crown ether coordination environment, the steric strain, that may build up between the ortho hydrogen atoms of the aniline ring and the ligand framework, was successfully eliminated, which in turn rendered ternary complex formation with solvent molecules thermodynamically unfavorable. Systematic optimization of the PET parameters was achieved by tuning the photophysical properties of the pyrazoline-based fluorophore and yielded a greater than 4000-fold fluorescence enhancement upon saturation with Mg (II). We anticipate that modification with hydrophilic substituents will also allow the design of high-contrast fluorescent probe for the selective detection of for alkaline earth metal ions in aqueous buffer. Most importantly, the previously identified challenges regarding ternary complex formation with Cu(I)-based probes[5] appears to equally apply towards other crown-ether based metal ion receptors. As demonstrated with this study, suppression of ternary complex formation combined with proper tuning of the photophysical characterisitics of the fluorophore may yield unusually high fluorescence contrast ratios for a broad range of fluorescent probes.

REFERENCES

1. Verma, Manjusha; Chaudhry, Aneese F.; Morgan, M. Thomas; Fahrni, Christoph J. "Electronically tuned 1,3,5-triarylpyrazolines as Cu(I)-selective fluorescent probes." *Org. Biomol. Chem.* (2010), *8*, 363-370.

2. Chaudhry, Aneese F.; Verma, Manjusha; Morgan, M. Thomas; Henary, Maged M.; Siegel, Nisan; Hales, Joel M.; Perry, Joseph W.; Fahrni, Christoph J. "Kinetically controlled photoinduced electron transfer switching in Cu(I)-responsive fluorescent probes.", *J. Am. Chem. Soc.* (2010), *132*, 737-747.

3. (a) Kavarnos, G. J., *Fundamentals of photoinduced electron transfer*. VCH Publishers: United States of America, 1993; (b) Fahrni, C. J., Design of cationselective synthetic fluorescent indicators in chemosensors, John Wiley & Sons, Inc.: 2011; pp 371-394.

4. (a) Verma, M.; Chaudhry, A. F.; Morgan, M. T.; Fahrni, C. J., "Electronically tuned 1,3,5-triarylpyrazolines as Cu(I)-selective fluorescent probes.*" Org. Biomol. Chem*. (2010), *8*, 363-370; (b) Cody, J.; Mandal, S.; Yang, L.; Fahrni, C. J., "Differential tuning of the electron transfer parameters in 1,3,5-triarylpyrazolines: a rational design approach for optimizing the contrast ratio of fluorescent probes." *J. Am. Chem. Soc*. (2008)**,***130* (39), 13023-13032; (c) Chaudhry, A. F.; Verma, M.; Morgan, M. T.; Henary, M. M.; Siegel, N.; Hales, J. M.; Perry, J. W.; Fahrni, C. J., "Kinetically controlled photoinduced electron transfer switching in Cu(I)-responsive fluorescent probes." *J. Am. Chem. Soc.* (2010), *132*, 737-747; (d) Fahrni, C. J.; Yang, L.; VanDerveer, D. G., "Tuning the photoinducd electron-transfer thermodynamics in 1,3,5-triaryl-2-pyrazoline fluorophores: X-ray structures, photophysical characterization, computational analysis, and in vivo evaluation." *J. Am. Chem. Soc.* (2003), *125*, 3799-3812; (e) Lin, J.; Rivett, D.; Wilshire, J., "The preparation and photochemical properties of some 1,3-Diphenyl-2-pyrazolines containing a heteroaromatic substituent." *Austr. J. Chem.* (1977*)***,** 30*, 629-637; (f) Rivett, D.; Rosevear, J.; Wilshire, J., "The preparation and spectral properties of some monosubstituted 1,3,5triphenyl-2-pyrazolines." *Austr. J. Chem.* (1979)**,** *32*, 1601-1612.

5. A. F. Chaudhry, S. Mandal, K. I. Hardcastle and J. Fahrni, "High-contrast Cu(I)-fluroescent probes based on synergistic electronic and conformational switching", *Chem. Sci.*, (2011), **2** 1016.

6. A. Ya. Freidzon, A. A. Bagatur'yants, S. P. Gromov, and M. V. Alfimov. "Recoordination of a metal ion in the cavity of a crown compound: a theoretical study. 1. Conformers of arylazacrown ethers and their complexes with Ca^{2+} cation", *Russ. Chem. Bull., Int. Ed.*, (2003), *52*, 2646-2655.